











Research Article

Impregnation of Silver Nanoparticles onto Polymers Based on Sugarcane Bagasse for the Remediation of Endocrine Disruptor–Bisphenol A from Water

Farid Mzee Mpatani ^{1,2} Ussi Makame Kombo ^{1,2} Khamis Rashid Kheir ^{1,2}
Nahya Khamis Nassor ² Daniel Joshua ² Salma Saleh Mussa ²
Salama Abubakar Mohamed ² Saide Abdulla Mbarak ^{1,2} Ali Shehe Hamad ²
and Salum Ali Ahmada ²

¹Chief Government Chemist Laboratory Agency (CGCLA), P.O. Box 759, Ministry of Health, Social Welfare, Elderly, Gender and Children, Zanzibar, Tanzania

²Zanzibar Health Research Institute (ZAHRI), P.O. Box 236, Ministry of Health, Social Welfare, Elderly, Gender and Children, Zanzibar, Tanzania

Correspondence should be addressed to Farid Mzee Mpatani; papilampatani@gmail.com

Received 18 August 2021; Revised 9 September 2021; Accepted 15 January 2022; Published 2 February 2022

Academic Editor: Chin Wei Lai

Copyright © 2022 Farid Mzee Mpatani et al. This is an open access article distributed under the Creative Commons Attribution License, which permits unrestricted use, distribution, and reproduction in any medium, provided the original work is properly cited.

This present study introduces a contemporary innovation of synthesized polymer–silver nanoparticle nanocomposite adsorbent based on sugarcane bagasse (AgNP-SB- β CD) for the sequestration of emerging micropollutant–bisphenol A from water matrix. Batch adsorption mode was carried out to assess the effectiveness of AgNP-SB- β CD nanocomposites towards eliminating bisphenol A (BPA). Characterization techniques including SEM, FTIR, and XRD have confirmed the successful incorporation of silver nanoparticles (AgNPs) onto bagasse–polymer. At 25°C, pH 7, and contact time of 120 min, the nanocomposites had a maximum uptake capacity of 158.4 mg g⁻¹ on BPA. The equilibrium isotherm of BPA on AgNPs-SB- β CD has fitted effectively with Langmuir model while the adsorption kinetics conformed to pseudo-second order. The adsorption phenomenon was controlled mainly by physisorption (via host–guest inclusion van der Waals bonding and pore filling effect). In addition, oxidative degradation of BPA by AgNPs-SB- β CD could marginally contribute the removal of BPA due to oxidative dissolution of AgNPs at pH 7. The thermodynamic results substantiate the spontaneity and exothermic behaviors of the adsorption phenomenon. The polymeric nanocomposite adsorbent was regenerated five times (using 75% ethanol) without considerable loss of its adsorption capacity. This authenticates its reusability and consistency performances; accordingly, it can be a market competitor adsorbent for the treatment of water contaminated with BPA.

1. Introduction

Water is amid the most fundamental natural resources in the life of living organisms, and therefore, it must be properly consumed to prevent future clean water scarceness [1, 2]. In recent decades, the incident of emerging micropollutants (EMPs), including bisphenol A (BPA) in water bodies, has become a growing concern due to their toxicological consequences on aquatic organisms, human health, and ecosystem [3–5]. For humans, the consumption of water tainted with

BPA can result a number of health complications including renal disorders [6], neurological problems, cardiovascular diseases, cancer, infertility, and sexual dysfunction [7].

BPA is among the primary manufactured and consumed chemicals worldwide [6, 8]. Since the last few decades, the utilization of BPA in the industries for the fabrication of epoxy resins and polycarbonate plastic products has been observed to augment significantly. This has led to generation of immense amount of BPA wastewaters from the industries. Intentionally, most of these wastewater effluents are released

to the environment without being completely treated; as a result, it causes adverse effects to the ecosystem [9].

As yet, several remediation techniques including adsorption [10–13], membrane process [14, 15], photocatalytic degradation [16, 17], and biological treatment process [18, 19] have been applied to treat water systems contaminated with BPA. Nonetheless, among these techniques, adsorption process has been regarded as a promising technology for effective remediation of wastewater polluted with BPA [20]. Adsorption technique possesses a facile, cost-effective and flexible operation, fast BPA removal, eco-friendly, and generates no indirect pollution [21–24].

In general, many researchers have focused on synthesized novel adsorbents as promising materials for remediation of water and wastewater to avoid human health complications and deterioration of the ecosystems [25]. Therefore, different adsorbents have been so far synthesized to adsorb BPA from water systems. These include the adsorbent based on natural materials, carbon and graphene, polymers, composite materials, nanomaterials, and agricultural waste materials [8]. However, a portion of adsorbents have demonstrated poor adsorptive and regeneration performances on bisphenol A [26], while some possess poor mechanical behaviors and are susceptible to extreme temperature and pH of the water surroundings. These limitations pose great challenges to the adsorbents for remediation of BPA and other noxious pollutants in water and wastewater. To surmount this challenge, in recent times, there has been an increasing concern on the application of polymer nanocomposite adsorbents (as a new class of adsorbents) for the treatment of noxious contaminants from aqueous systems. These advanced polymer nanocomposites are economical, highly stable, and effective adsorbents on removing a broad spectrum of chemical and biological pollutants [27]. They possess beneficial characteristics including dimensional flexibility, functionalities, film forming capability [28], medium mobility, porosity behaviors, and sturdy mechanical characteristics [29–31]. Thus, in this present research, we have reported for the first time the amalgamation of silver nanoparticles onto polymers based on sugarcane bagasse and applied for the sequestration of emerging micropollutant–bisphenol A from water. Incorporation of silver nanoparticles was done to increase the surface features, stability, and functional moieties on bagasse–polymers, whereby all these properties are accountable for increasing the uptake of bisphenol A.

Herein, the colloidal silver nanoparticles (AgNPs) were synthesized using reduction method, and then, a wet impregnation protocol was performed to immobilize AgNPs onto bagasse– β -cyclodextrin polymer to form novel bagasse–polymer–silver nanoparticle nanocomposites (AgNP-SB- β CD). These nanocomposites were characterized using various analytical techniques and then assessed their adsorptive performance towards bisphenol A in water matrix.

2. Materials and Methods

2.1. Materials. Pristine sugarcane bagasse material (SB) was obtained from Zanzibar Sugar Factory Limited (ZSFL) Mahonda, Tanzania, and used as a starting material for synthesized polymeric nanocomposites. Bisphenol A (BPA,

$C_{16}H_{18}O_2$, 228.29 g mol⁻¹), silver nitrate (AgNO₃, 169.87 g mol⁻¹), beta-cyclodextrin (β -CD, 1134.98 g mol⁻¹), citric acid (CA, 192.12 g mol⁻¹), poly(*N*-vinyl pyrrolidone) (PVP), hydrazine monohydrate (N₂H₄·H₂O, 50.06 g mol⁻¹), calcium chloride (CaCl₂, 110.98 g mol⁻¹), sodium hydroxide (NaOH, 39.997 g mol⁻¹), absolute ethanol (CH₃CH₂OH, 46.07 g mol⁻¹), sodium sulfate (Na₂SO₄, 142.04 g mol⁻¹), hydrochloric acid (HCl, 36.458 g mol⁻¹), and sodium dihydrogen phosphate (NaH₂PO₄, 119.98 g mol⁻¹) were used in this study. All chemicals and standard solutions were of highest purity and applied as delivery without additional modification and were purchased from Macklin Biochemical Co., Ltd (Shanghai, China), Loba Chemie Pvt. Ltd (Mumbai, India), Kas Medics Ltd, and Lab Equip Ltd (Dar es Salaam, Tanzania).

2.2. Preparation of the Novel Bagasse–Polymer–Silver Nanoparticle Nanocomposites and Bisphenol A Solution. Optimization protocols were implemented to synthesize bagasse–polymer–silver nanoparticle nanocomposite (AgNP-SB- β CD) adsorbent. Herein, sugarcane bagasse (SB) material was thoroughly cleaned with water to eliminate unwanted materials and then rinsed with distilled water to remove other inorganic impurities. The clean SB was cured for over 12 h at 60°C and then milled to particle size of 150 μ m. An accurate 1.5 g of SB was placed in vessel containing a solution mixture prepared by mixing CA (4.5 g), β -CD (9.0 g), and NaH₂PO₄ (0.95 g) in 200 mL of distilled water. The mixture was agitated and cured at 180°C for 30 min to obtain bagasse- β -cyclodextrin (SB- β CD) polymers as explained by Mpatani et al. [26]. Then, preparation of colloidal silver nanoparticles (AgNPs) by reduction method was performed in fume hood with minor modification as described by Abdelwahab and Shukry [32]. 0.08 mol L⁻¹ of AgNO₃ solution was prepared and added (while stirring) to a solution obtained by incorporating 1.0 g of PVP into 200 mL of ethanol. Then, N₂H₄·H₂O solution (0.02 mol L⁻¹) was added in drops with constant stirring to the solution containing AgNO₃ and PVP. The solution was altered to pH 8 by 0.1 mol L⁻¹ NaOH. Then, the formed solution was cured at 60°C under constant stirring till the solution color changed to yellow (AgNP colloidal solution). The SB- β CD polymer material was then introduced into colloidal solution and agitated at 120 rpm for overnight to allow sufficient amalgamation of AgNPs into polymer network of SB- β CD. The resulting polymeric nanocomposites were then filtered and cleaned with distilled water and cured at 60°C for 4 h. The AgNP-SB- β CD nanocomposite adsorbent was then stored in the container and used for adsorption process.

A concentrated solution of bisphenol A (BPA, 1000 mg L⁻¹) was prepared by placing 1 g of BPA into a 1 L graduated flask containing a methanol:water solution (1:1 ratio). BPA working solutions were obtained by diluting a concentrated BPA solution using distilled water to the desirable concentration. BPA solutions were regulated to pH of 2.0 to 11.0 using 0.1 mol L⁻¹ of HCl or NaOH solution.

2.3. Characterizations of Polymeric Nanocomposite Adsorbent. The physicochemical properties of the novel bagasse–polymer–silver nanoparticle nanocomposite

(AgNP-SB- β CD) adsorbent were characterized with point of zero charge (pH meter, Mettler Toledo FP30-standard), Fourier-Transform Infrared Spectroscopy (FTIR, Laser class 1 Bruker Alpha with ATR), X-ray diffraction (XRD, Inxitu BTX-231 Benchtop), scanning electron microscopy (SEM, JSM-7600F Thermo NORAN System7), and Brunauer-Emmett-Teller technique (Quantachrome NOVA 4200e BET Analyzer, UK).

2.4. Batch Adsorption Experiments. An assortment of adsorption factors including solution pH, adsorption temperature, adsorbent dose, contact time, salt concentration, and regeneration study was performed to assess the steadiness and adsorption capacity of AgNPs-SB- β CD towards removing bisphenol A. Batch adsorption experiments were done by considering three approaches: (i) the use of different temperatures (25, 35, and 45°C) at constant BPA concentration (100 mg L⁻¹) and AgNP-SB- β CD dose (0.01 g), (ii) the use of different AgNP-SB- β CD doses (0.0025, 0.005, 0.01, 0.015, and 0.02 g) at constant BPA concentration (100 mg L⁻¹) and temperature (25°C), and (iii) the use of different BPA concentrations (25–200 mg L⁻¹) at stable temperature (25°C) and AgNP-SB- β CD dose (0.01 g). CaCl₂ and Na₂SO₄ solutions (0–0.1 mol L⁻¹) were employed to examine the influence of ionic strength (salt concentration) on uptake of bisphenol A. All adsorption experiments were performed in water bath shaker at rotation speed of 140 rpm using different contact time (5, 10, 15, 30, 45, 60, and 120 min). At given time, the concentration of BPA in the supernatant sample was measured at 276 nm using a UV-Vis spectrophotometer (Hewlett-Packard Co. Palo Alto). The adsorption capacity (q_e) and removal efficiency (% P) of bisphenol A at equilibrium were calculated from Equations (1) and (2), respectively.

$$q = \frac{V(C_0 - C_e)}{m}, \quad (1)$$

$$P = \frac{(C_0 - C_e)}{C_0} \times 100\%. \quad (2)$$

In general, 0.01 g of AgNP-SB- β CD nanocomposites, 100 mg L of BPA, 10 mL of BPA, pH 7.0, adsorption temperature of 25°C, and contact duration of 120 min were used as the optimal experimental parameters for adsorption and regeneration studies.

2.4.1. Kinetic and Isotherm Determination. Adsorption isotherm and kinetic can assist in understanding the adsorption affinity, surface chemistry of the adsorbent, the rate, and mechanisms that control adsorption phenomenon [33]. Herein, pseudo-first-order (PFO) and pseudo-second-order (PSO) models were employed to determine the kinetic study, while Freundlich and Langmuir models were employed to evaluate the equilibrium isotherms [1, 34]. The expressions of isotherm and kinetic models are presented in Table 1.

2.4.2. Thermodynamic Approach. The domination of temperature on BPA uptake was examined at 25, 35, and 45°C. This thermodynamic study can help to understand the

adsorption behavior, interaction, and mechanisms involved [26]. The Gibbs free change (ΔG^0), change in entropy (ΔS^0), and standard enthalpy of the reaction (ΔH^0) were resolute using the subsequent equations.

$$K_d = \frac{q_e}{C_e}, \quad (3)$$

$$\Delta G^0 = -RT \ln K_d, \quad (4)$$

$$\ln K_d = \frac{-\Delta H^0}{RT} + \frac{\Delta S^0}{R}, \quad (5)$$

where K_d (L mg⁻¹) is the partition coefficient of the least BPA concentration, q_e (mg g⁻¹) is the uptake capacity at equilibrium, C_e (mg L⁻¹) is the equilibrium mass concentration of the BPA, T (K) is the adsorption temperature, and R (8.314 J mol⁻¹ K⁻¹) is the molar gas constant. The Van't Hoff equation (Equation (5)) was employed to find ΔS^0 and ΔH^0 from the intercept and slope by sketching a graph of $\ln K_d$ versus $1/T$.

2.5. Regeneration Approaches. Three desorption solutions (0.1 M NaOH, 0.1 M HCl, and 75% ethanol) were used to assess the adsorption performance (effectiveness, firmness, and reusability) of nanocomposite adsorbent towards decontaminating bisphenol A from water systems. Desorption-regeneration analysis is one of the important adsorption procedures which can be applied to define the economical and environmental perspective of the adsorbent [35]. In this study, desorption and regeneration procedures were carried out in quintuplicate. 0.01 g of AgNP-SB- β CD adsorbent was put into 50 mL Erlenmeyer flask having 10 mL of 100 mg L⁻¹ BPA solution with pH 7.0 and agitated at 140 rpm for 120 min. After equilibrium time (120 min), the nanocomposite adsorbent loaded with BPA was then separated by centrifugation and thoroughly washed with distilled water and dried up at 60°C for 8 h. A dried AgNP-SB- β CD was weighed up and put into Erlenmeyer flask having 10 mL of desorption solution. The flask was shaken in a water bath with rotation speed of 140 rpm at 25°C for 120 min. AgNP-SB- β CD sample was centrifuged, cleaned with distilled water, and cured at 60°C for 8 h. The desorption solution containing BPA was then measured at 276 nm to calculate the BPA concentration desorbed. These approaches were carried out independently to all desorption solutions (0.1 M NaOH, 0.1 M HCl, and 75% ethanol). The desorption effectiveness (d) and regeneration effectiveness (r) of AgNPs-SB- β CD were calculated from Equations (6) and (7), respectively.

$$d = \frac{m_d}{m_0} \times 100\%, \quad (6)$$

$$r = \frac{q_d}{q_0} \times 100\%, \quad (7)$$

where m_d is the weight (g) of AgNPs-SB- β CD desorbed, m_0 (g) is the weight of the BPA left over on the AgNPs-SB- β CD before desorption, q_0 (mg g⁻¹) is the uptake capacity of

TABLE 1: The expressions of isotherm and kinetic models applied to examine the uptake of bisphenol A onto AgNP-SB- β CD nanocomposites.

Model	Equation	Description
Pseudo-first order	$q_t = q_e(1 - e^{-k_1 t})$	k_1 (min^{-1}) is the specific rate constant of PFO; q_e or q_t (mg g^{-1}) are the uptake capacity at equilibrium or any time t .
Pseudo-second order	$q_t = k_2 q_e^2 t / 1 + k_2 q_e t$	k_2 ($\text{g mg}^{-1} \text{min}^{-1}$) is the PSO reaction rate coefficient.
Langmuir	$q_e = q_m K_L C_e / 1 + K_L C_e$	q_m is the highest uptake capacity (mg g^{-1}); K_L is associated to the adsorption attraction of the binding energy (L mg^{-1}).
Freundlich	$q_e = K_F C_e^{1/n}$	K_F is the Freundlich constant ($\text{mg g}^{-1} / (\text{mg L}^{-1})^n$) and $1/n$ is the heterogeneity factor indicating the affinity of the BPA to the AgNP-SB- β CD nanocomposite.

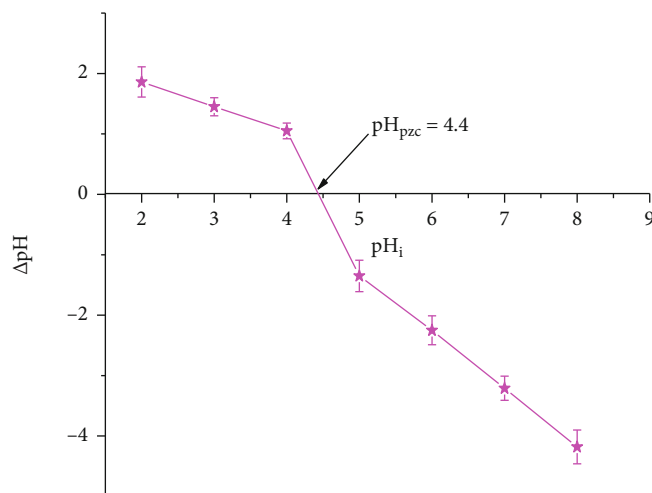


FIGURE 1: Point zero charge of AgNP-SB- β CD nanocomposites.

AgNPs-SB- β CD in the initial running experiment, q_n (mg g^{-1}) is the uptake capacity of AgNPs-SB- β CD after reused, and n is the sum total of regeneration cycles performed.

2.6. Statistical Data Approach. Adsorption isotherm and kinetic results were accomplished using nonlinear regression in Origin 8.5.1. Microsoft excel 2016 was applied in advance to analyze the data. All tests were carried out in triplicates (with the exception of regeneration analysis which was done in quintuplicate), and the results were expressed as mean \pm standard error.

3. Results and Discussion

3.1. Characterization of AgNP-SB- β CD Nanocomposite Adsorbent. Taking into consideration that adsorption process is a surface incident, the nature of surface chemistry and structure of adsorbent can considerably influence the uptake of pollutants from water systems. The possession of surface features (such as functional groups, pores, particle sizes, and higher surface area) on adsorbent can attribute to the removal of BPA [20]. Herein, characterization of AgNP-SB- β CD nanocomposites was performed, and the results obtained are discussed as follows:

3.1.1. Point of Zero Charge. Determination of adsorbent point zero charge (pH_{pzc}) is imperative as it helps to under-

stand the surface charge of adsorbent and an appropriate pH medium that suit adsorption process [1]. Analysis of pH_{pzc} of AgNPs-SB- β CD was carried out with some modification using drift method as described by Doczekalska et al. [36]. As shown in Figure 1, AgNP-SB- β CD nanocomposites have pH_{pzc} of 4.4. This indicated that, at pH solution $< \text{pH}_{\text{pzc}}$ (acidic medium), the AgNP loaded onto nanocomposites destabilized and aggregates causing lower uptake of BPA. However, at pH solution $> \text{pH}_{\text{pzc}}$, the embedded AgNPs existed into two forms: oxidative dissolution state at neutral pH medium or stable suspension at alkaline condition [37, 38]. The AgNPs-SB- β CD in the neutral pH solution had higher removal capacity towards BPA due to the occurrence of both adsorption and oxidative degradation of BPA.

3.1.2. FTIR Examination. FTIR analysis was carried out to identify the functional groups that are accountable for adsorption of bisphenol A onto polymeric nanocomposites. The change of band position and intensities of SB- β CD polymer after impregnation process were considered to confirm the successful incorporation of AgNPs onto bagasse-polymer. As appeared in Figure 2, the band intensity of AgNP-SB- β CD spectrum had lessened due to the integration of AgNPs. Moreover, the peak corresponding to the stretching vibration of -OH has slightly decreased from 3420 cm^{-1} (SB- β CD) to 3410 cm^{-1} (AgNPs-SB- β CD). This suggests that there was an interaction (during

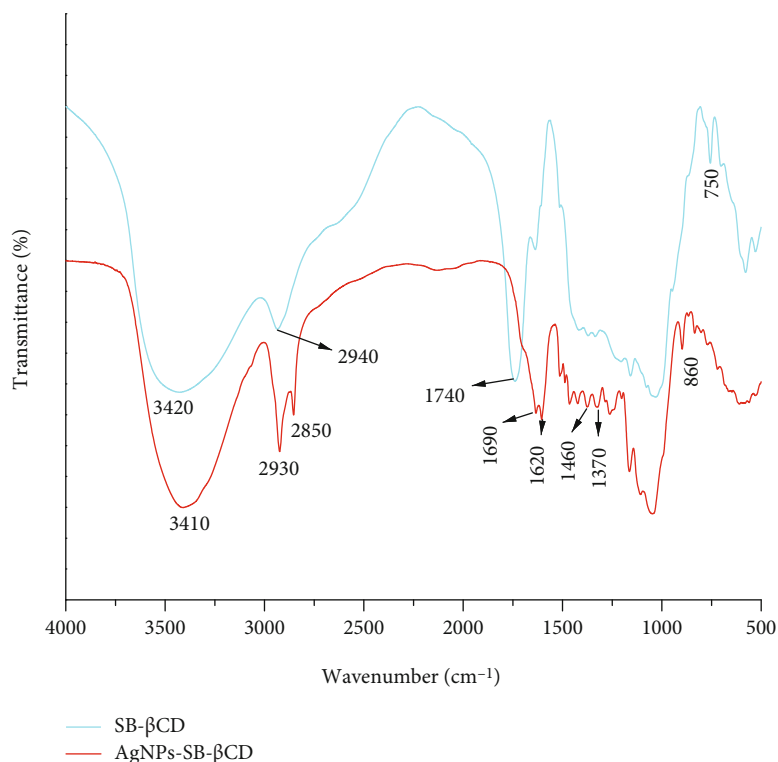


FIGURE 2: FTIR spectra of SB-βCD polymer and AgNP-SB-βCD nanocomposites.

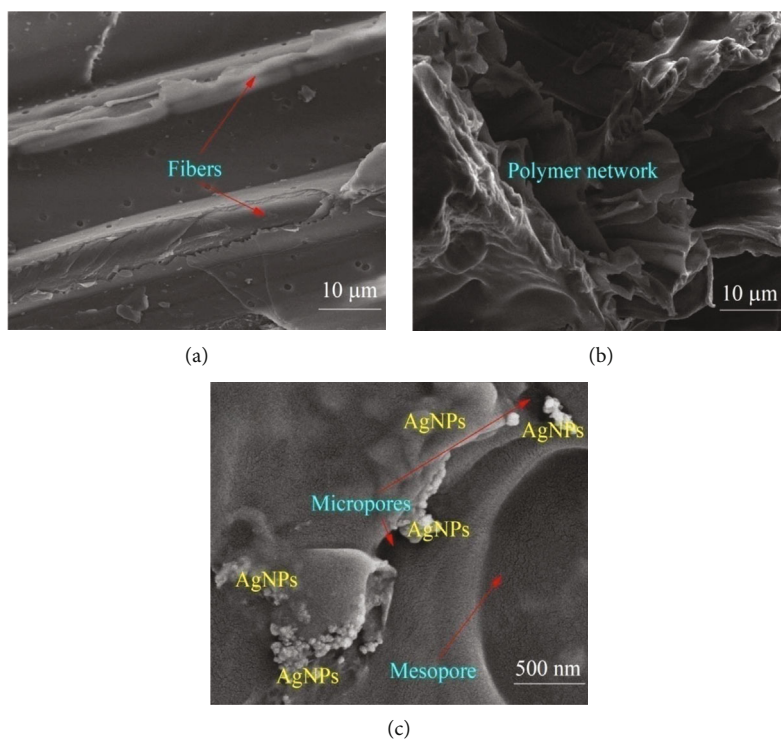


FIGURE 3: Scanning electron microscopy pictures present the morphology of (a) raw SB, (b) SB-βCD polymers, and (c) AgNP-SB-βCD nanocomposites.

impregnation process) between the bagasse-polymers' hydroxyl groups and AgNPs to form linkages. In addition, the new peaks on AgNP-SB-βCD spectrum at 2930, 2860,

1690, 1620, 1460, 1370, and 860 cm^{-1} designating the existence of silver nanoparticles capped on the surface of bagasse-polymer [39].

TABLE 2: Textural characteristics of a novel bagasse–polymer–silver nanoparticle nanocomposite (AgNP-SB- β CD) adsorbent.

Nanocomposite adsorbent	S_{BET} (m^2g^{-1})	V_M (cm^3g^{-1})	D_p (nm)	V_T (cm^3g^{-1})
AgNPs-SB- β CD	20.83	0.022	15.4	0.061

S_{BET} : BET surface area; V_M : micropore volume; D_p : pore diameter; V_T : total pore volume.

3.1.3. SEM and BET Examination. Scanning electron microscopy images of SB, SB- β CD, and AgNPs-SB- β CD are presented in Figure 3. The surface morphology of SB is appeared to be smooth with parallel fibers connected with pith. However, after being crosslinked with β -cyclodextrin, the SB- β CD became irregular, cracked, and possessed polymer networks. The amalgamation of silver nanoparticles with SB- β CD had resulted the formation of nanocomposites (AgNPs-SB- β CD) that have the surface area, average pore size, and total pore volume of $20.83\text{ m}^2\text{g}^{-1}$, 15.4 nm , and $0.061\text{ cm}^3\text{g}^{-1}$, respectively (Table 2). The AgNPs seem to increase the pore volume, surface area, and pore size of bagasse–polymer. As reported by Mpatani et al. [26], SB- β CD polymer adsorbent had a respective pore size, surface area, and pore volume of 9.28 nm , $8.56\text{ m}^2\text{g}^{-1}$, and $0.0434\text{ cm}^3\text{g}^{-1}$. As seen in Figure 3, the AgNPs are scattered and clustered on the surface of AgNPs-SB- β CD. This means that during impregnation process, AgNPs were diffused on the surface of bagasse–polymer, breaking the fibrous network of cellulose, dispersed in the polymer network, and resulting bond formation between AgNPs and bagasse–polymer. These interaction phenomena have led to development of mesopores, micropores, and cracks. The nanostructure of AgNPs together with the bond-breaking-bond-forming phenomenon could contribute to the increasing of total pore volume and surface area of AgNPs-SB- β CD. These interaction incidents are consistent with the results reported by Trinh et al. [40].

3.1.4. XRD Analysis. As seen in Figure 4, the peak intensity of SB- β CD polymer adsorbent has increased after being impregnated with silver nanoparticles (AgNPs). Besides, the position of diffraction peak at 19.2° that attributed to amorphous nature of SB- β CD polymer had slightly shifted to 20.4° after impregnation process. In addition, three new peaks were formed at 35.5 , 43.6 , and 63.7° which are, respectively, attributed to crystal plane (111), (200), and (220) of cubic Ag nanoparticles [41]. These AgNPs have relative influences on altering bagasse–polymer signals. The shift of the peak (from 19.2 to 20.4°), development of new peaks (35.5 , 43.6 , and 63.7°), and formation of crystalline nature of AgNPs-SB- β CD confirm the successful incorporation of silver nanoparticles onto cyclodextrin polymer based on sugarcane bagasse.

3.2. Batch Adsorption Studies

3.2.1. Contribution of Contact Time on BPA Uptake. Adsorption experiments were conducted to assess the influence of contact duration on the uptake of 100 mg L^{-1} BPA onto

AgNPs-SB- β CD. At both temperatures, the adsorption equilibrium for the uptake of BPA was attained within 120 min (Figure 5). However, approximately half of adsorptive–oxidative capacity of AgNPs-SB- β CD on BPA has been achieved in the first 5 min, and afterward, the uptake became slowly increased until the equilibrium was reached. At 25°C , 40.3 , and 75.2% of 100 mg L^{-1} BPA was eliminated from the solution at 5 and 120 min. This means that the active sites of AgNPs-SB- β CD (through adsorption and oxidation processes) were more accessible at the beginning of contact process and then became occupied as the time goes.

Pseudo-first-order and pseudo-second-order models were regarded to give the kinetic information on the removal of BPA using AgNPs-SB- β CD. The values obtained from the determined coefficient (R^2), chi-square statistics (χ^2), and calculated adsorption capacity ($q_e\text{ calc.}$) were considered to determine the best fitted kinetic model. The kinetic model data and plotted curves are presented in Table 3 and Figure 5, respectively. As it can be seen in Table 3, the calculated q_e obtained from pseudo-second-order model at 25 , 35 , and 45°C were moderately similar with experimental q_e . Moreover, the values of coefficient of determination (R^2) of pseudo-second-order model were higher ($R^2 > 0.98$) compared to that of pseudo-first-order ($R^2 < 0.89$). In addition, the chi-square statistics (χ^2) values from the pseudo-second-order model were relatively smaller, and the plotted curves were closer to experimental points. This implied that the adsorption kinetics for the uptake of BPA onto AgNPs-SB- β CD was governed by PSO reaction.

3.2.2. Contribution of BPA Concentration on Adsorption Capacity of AgNPs-SB- β CD and Isotherm Studies. The sequestration of bisphenol A using 0.01 g of AgNPs-SB- β CD was assessed at different mass concentrations of BPA (25 , 50 , 75 , 100 , 125 , 150 , 175 , and 200 mg L^{-1}) and temperatures (25 , 35 , and 45°C). The deviation between the uptake capacity (q_e) and equilibrium concentration (C_e) is shown in Figure 6. At individual temperature, the uptake of BPA onto AgNPs-SB- β CD was steadily improved with the increase of bisphenol A concentration till the highest uptake capacity of AgNPs-SB- β CD was reached. Increasing of BPA concentration seemed to facilitate the interaction between AgNPs-SB- β CD and BPA molecules. These results are comparable with the findings described by Han et al. [42] and Aryee et al. [43].

In this study, the adsorption isotherm data were fit to Freundlich and Langmuir models using nonlinear regression analysis. The chi-square statistics (χ^2), coefficient of determination (R^2), separation factor (R_L), and fitted curves were considered mostly to predict the best isotherm model that governed adsorption phenomenon. It is apparent that the experimental data on the fitted curves are much closer for Langmuir than Freundlich model (Figure 6). Moreover, Langmuir model had higher coefficient of determination ($R^2 > 0.991$) and lower chi-square statistics ($\chi^2 < 1.3$) at both temperatures compared to Freundlich model ($R^2 < 0.970$ and $\chi^2 > 4.1$) (Table 4). In addition, the R_L values calculated from initial concentration of BPA ($C_0 = 100\text{ mg L}^{-1}$) were

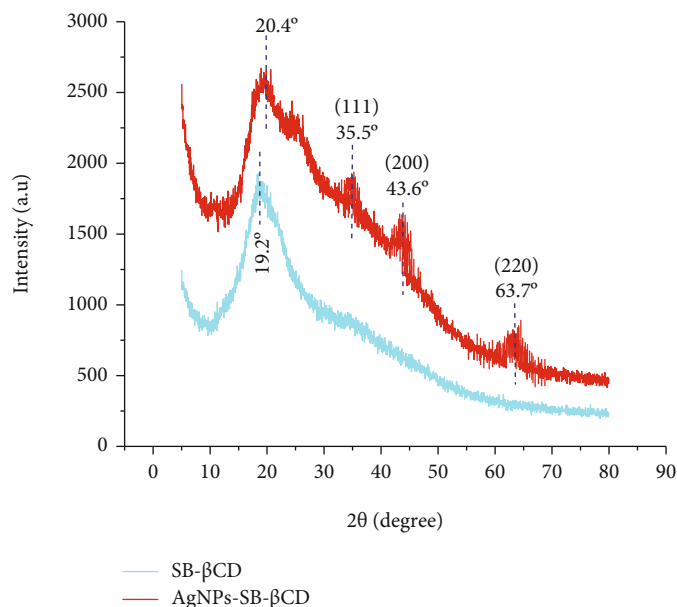


FIGURE 4: X-ray diffraction pattern of SB- β CD polymers and AgNP-SB- β CD nanocomposites.

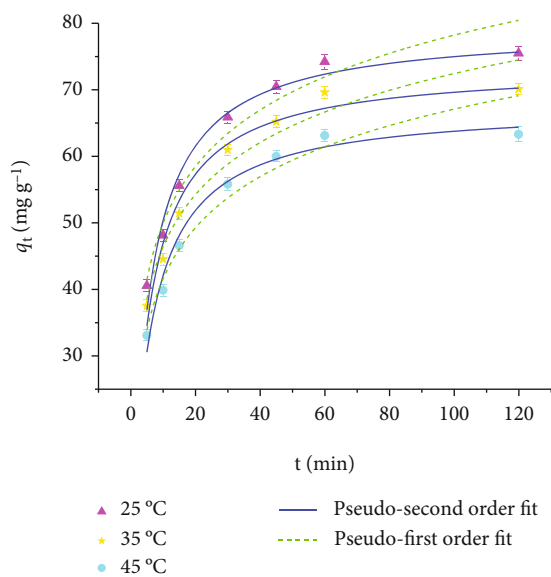


FIGURE 5: Contact duration influence on uptake of BPA onto AgNP-SB- β CD nanocomposites ($C_0 = 100 \text{ mg L}^{-1}$, $V = 10 \text{ mL}$, and $m = 0.01$).

less than unit ($R_L < 1$). These results confirm that adsorption isotherm is well governed by Langmuir model, and monolayer adsorption was occurred on the uniform surface of AgNPs-SB- β CD.

In this present study, the maximum adsorption uptake of AgNPs-SB- β CD for bisphenol A at 25, 35, and 45°C is 158.4, 149.1, and 141.2 mg g^{-1} (Table 4). By comparing from the study of Mpatani et al. [26], the adsorption capacity of bagasse-polymer towards BPA (at 25°C) has improved from 121 mg g^{-1} (SB- β CD) to 158.4 mg g^{-1} (AgNPs-SB- β CD) after amalgamation process. This increasing of adsorption capac-

ity is due to the incorporation of AgNPs that led the improvement of surface features and functional moieties on the bagasse-polymer, whereby all these together brought adsorption and oxidation processes on BPA. In addition, these polymeric nanocomposites (AgNPs-SB- β CD) have demonstrated stability and reusability behaviors and possess higher removal capacity compared with a number of adsorbents (including 2-vinylpyridine functionalized magnetic nanoparticle, modified carbon nanotubes, magnetic nanoparticles, alfafa-derived biochar, molecularly imprinted polymer, bagasse-polymer, and CTAB-walnut shell) reported from the previous studies on removal of BPA from water system (Table 5). Therefore, there is market competent on AgNPs-SB- β CD for BPA wastewater remediation.

3.2.3. Contribution of pH Solution on BPA Uptake. The pH solution had a major influence on the characteristics of bagasse-polymer-silver nanoparticle nanocomposites (AgNP-SB- β CD) on removing BPA. The removal efficiency of AgNPs-SB- β CD was lower at both acidic and alkaline media (Figure 7). This might be elucidated by the, respectively, existence of AgNPs in aggregation and stable suspension states [38], whereby the removal of BPA was mostly governed by adsorption process through host-guest inclusion and pore diffusion mechanisms. However, at neutral medium, the uptake of BPA onto AgNPs-SB- β CD was much enhanced due to the dissolution of AgNPs which brought degradation of BPA. In this circumstance, the interaction of BPA and nanocomposites was managed by both adsorption and oxidative degradation processes, consequently resulted higher removal of BPA from water solution.

3.2.4. Contribution of AgNP-SB- β CD Dosage on BPA Uptake. The impact of nanocomposite dosage on BPA removal was carried out by altering AgNP-SB- β CD mass and maintains other factors constant. Different masses of

TABLE 3: Kinetic data for the uptake of BPA onto AgNP-SB- β CD nanocomposites.

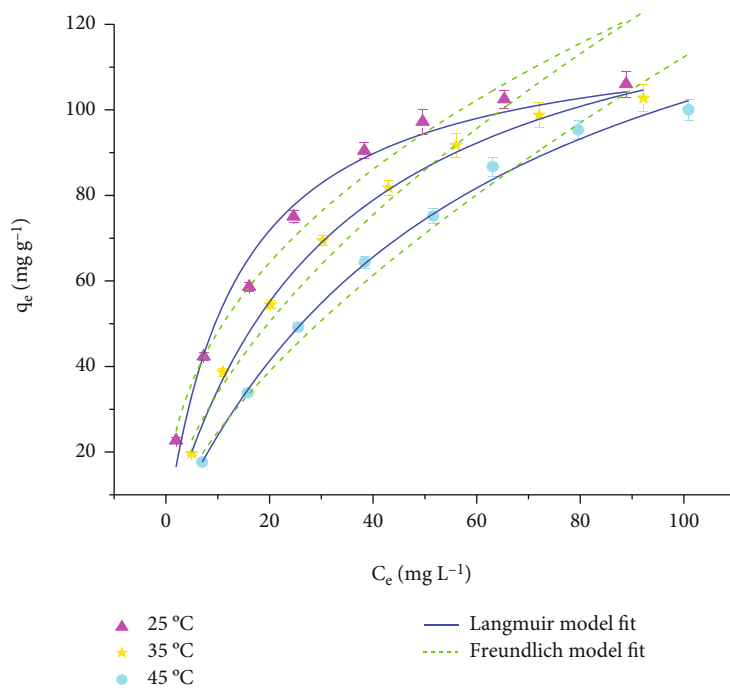
(a)

Temperature/ $^{\circ}$ C	$q_{e(\text{meas})}$ (mg g^{-1})	PFO model $q_{e(\text{theo})}$ (mg g^{-1})	$k_1 \times 10^{-1}$ (min^{-1})	R^2	χ^2
25	75.2 ± 2.2	66.2 ± 5.7	1.27 ± 0.18	0.879	20.54
35	69.6 ± 1.7	58.1 ± 4.9	1.16 ± 0.16	0.872	25.76
45	64.5 ± 2.6	52.6 ± 3.6	1.06 ± 0.15	0.845	27.68

(b)

Temperature/ $^{\circ}$ C	$q_{e(\text{meas})}$ (mg g^{-1})	PSO model $q_{e(\text{theo})}$ (mg g^{-1})	$k_2 \times 10^{-3}$ ($\text{g mg}^{-1} \text{min}^{-1}$)	R^2	χ^2
25	75.2 ± 2.2	77.5 ± 1.8	2.19 ± 0.28	0.989	3.95
35	69.6 ± 1.7	71.4 ± 1.6	2.26 ± 0.25	0.991	2.94
45	64.5 ± 2.6	66.1 ± 1.4	1.95 ± 0.17	0.992	2.52

$\chi^2 = \sum (q_{e(\text{meas})} - q_{e(\text{theo})})^2 / q_{e(\text{theo})}$, where $q_{e(\text{meas})}$ and $q_{e(\text{theo})}$ are experimental measured and theoretical calculated adsorption capacities, respectively.

FIGURE 6: Adsorption equilibrium isotherms of BPA onto AgNP-SB- β CD nanocomposites.

AgNPs-SB- β CD (0.0025, 0.005, 0.01, 0.015, and 0.02 g) were put individually into Erlenmeyer flask containing 100 mg L^{-1} , and then, adsorption process was done at 25°C . At equilibrium, the uptake capacity (q_e) of AgNPs-SB- β CD towards 100 mg L^{-1} of BPA was appeared to diminish from 197.2 to 46.8 mg g^{-1} , while the removal effectiveness (% P) increased from 49.3 to 93.7% with the raise of nanocomposite dosage from 0.0025 to 0.02 g (Figure 8). The higher uptake capacity (q_e) was achieved when the AgNP-SB- β CD dosage was low. This is because at higher dosage, most of the active sites become vacant, resulting lower BPA uptake. The same facts have been described in the studies by Ponnusami et al. [48], Mpatani et al. [26], and Kani et al. [49].

3.2.5. Influence of Cations and Anions on BPA Uptake. Usually, the wastewater influents generated from the industries are accompanied with enormous amount of ions. These ions may greatly affect the performance of adsorbent for removing designated pollutants. Therefore, assessing the influence of coexisting ions on BPA uptake onto AgNPs-SB- β CD is of compulsory. The findings of this present study demonstrate that the presence of CaCl_2 in the water system can affect the uptake capacity of AgNPs-SB- β CD on BPA. At 25°C , the initial uptake capacity (75.2 mg g^{-1}) of AgNPs-SB- β CD had decreased to 60.8 and 50.7 mg g^{-1} when a respective CaCl_2 concentration of 0.02 and 0.1 mol L^{-1} was used. Both coexistence ions (Ca-cations and Cl-anions) had positive effects of

TABLE 4: The data of isotherm model parameters obtained on adsorption of BPA by AgNPs-SB- β CD.

Model	Parameters	Temperature/ $^{\circ}$ C		
		25	35	45
Langmuir	q_m (mg g^{-1})	158.4 ± 5.1	149.1 ± 4.3	141.2 ± 7.5
	K_L (L mg^{-1})	0.0176 ± 0.003	0.0296 ± 0.001	0.062 ± 0.005
	R^2	0.994	0.999	0.997
	R_L	0.362	0.253	0.138
	χ^2	1.273	0.144	0.584
Freundlich	$1/n$	0.416 ± 0.027	0.519 ± 0.032	0.574 ± 0.028
	K_F [$(\text{mg L}^{-1})(\text{L mg}^{-1})^{1/n}$]	18.81 ± 1.91	11.19 ± 1.33	7.44 ± 1.15
	R^2	0.962	0.958	0.954
	χ^2	4.454	4.263	5.851

$R_L = 1/(1 + K_L C_0)$ where R_L is the separation factor and C_0 is the initial concentration of BPA (100 mg L^{-1}).

TABLE 5: Adsorption performance of different adsorbents towards bisphenol A removal.

Adsorbent	pH	Temperature/K	$q_e/(\text{mg g}^{-1})$	Reference
AgNPs-SB- β CD	7.0	298	158.4	This study
2-Vinylpyridine functionalized magnetic nanoparticle	6.0–7.0	293	115.9	[10]
Modified carbon nanotubes	6.0	280	70	[44]
SB- β CD	7.0	298	121	[26]
Magnetite nanoparticles	6.0	303	4.785	[45]
Molecularly imprinted polymer	—	298	40.31	[46]
CTAB-walnut shell	6.0	303	38.5	[13]
Alfa-derived biochar (AF 650)	6.0	295	38	[47]

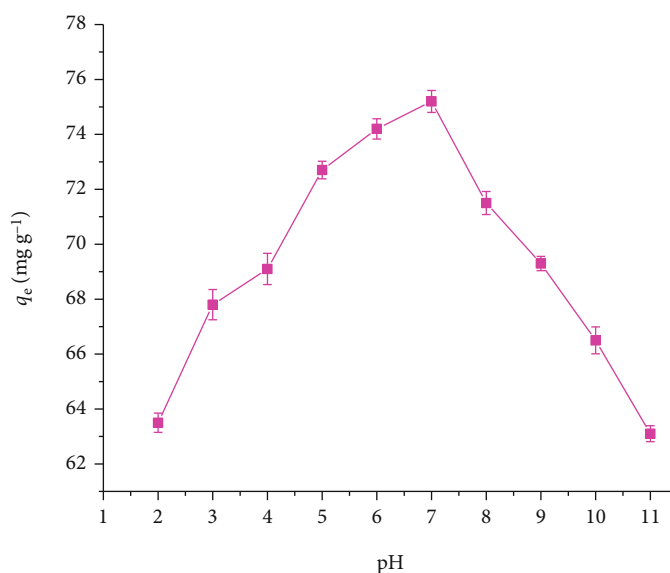


FIGURE 7: Solution pH impact on uptake of bisphenol A onto AgNP-SB- β CD nanocomposites ($C_0 = 100 \text{ mg L}^{-1}$, $V = 10 \text{ mL}$, $m = 0.01 \text{ g}$, $T = 25^{\circ}\text{C}$, and $t = 120 \text{ min}$).

adsorption process. Ca^{2+} ions have affinity of resulting complex formation with AgNPs-SB- β CD via interaction with β CD cavities. This incident can reduce the adsorption performance by lessening the adsorption sites of AgNPs-SB- β CD for adsorbing BPA. The same phenomenon was

reported by Mpatani et al. [26] on SB- β CD polymer adsorbent. At the same time, the Cl^{-} ions in solution can act as inorganic ligands that strongly have affinity to oxidized AgNPs into dissolution state [50, 51] and resulting oxidative degradation of BPA. However, since adsorption incident

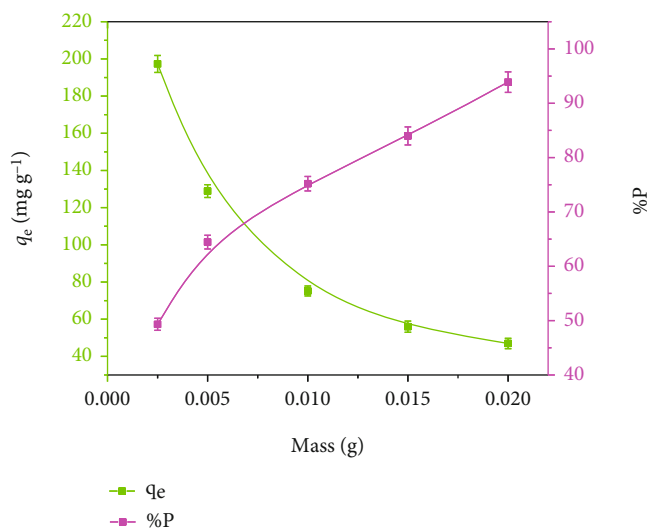


FIGURE 8: Influence of AgNP-SB- β CD dosage on uptake of BPA at 25°C.

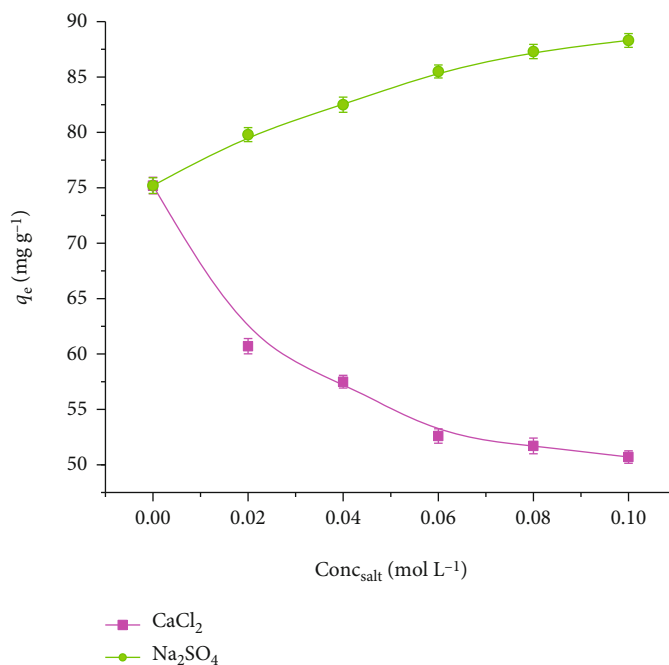


FIGURE 9: Influence of ion interference on uptake of BPA onto AgNP-SB- β CD nanocomposites ($C_0 = 100 \text{ mg L}^{-1}$, $V = 10 \text{ mL}$, $m = 0.01 \text{ g}$, $T = 25^\circ\text{C}$, and $t = 120 \text{ min}$).

(through β CD cavities and mesopores) contributed much for the uptake of BPA onto AgNPs-SB- β CD than oxidative degradation (through AgNPs), therefore the adsorption capacity of AgNPs-SB- β CD was reduced in the presence of CaCl_2 (Figure 9).

On the other side, the existence of Na_2SO_4 had a positive effect of increasing the AgNP-SB- β CD capacity for eliminating BPA. According to the findings by Mpatani et al. [26], Na_2SO_4 has a tendency of diminishing BPA solubility in the solution; as a result, more BPA can be taken onto AgNPs-SB- β CD through host-guest inclusion, pore filling effect, and

TABLE 6: Thermodynamic data on elimination of bisphenol A onto AgNPs-SB- β CD.

25°C	$\Delta G^0/(\text{kJ mol}^{-1})$			$\Delta H^0/(\text{kJ mol}^{-1})$	$\Delta S^0/(\text{J mol}^{-1} \text{K}^{-1})$
	35°C	45°C			
-5.83	-3.41	-2.38	-57.4	-173.7	

oxidative degradation process. At 25°C, the initial adsorption capacity of AgNPs-SB- β CD (75.2 mg g^{-1}) had escalated to 79.8 and 88.3 mg g^{-1} when a particular Na_2SO_4 concentration of 0.02 and 0.1 mol L^{-1} was introduced (Figure 9).

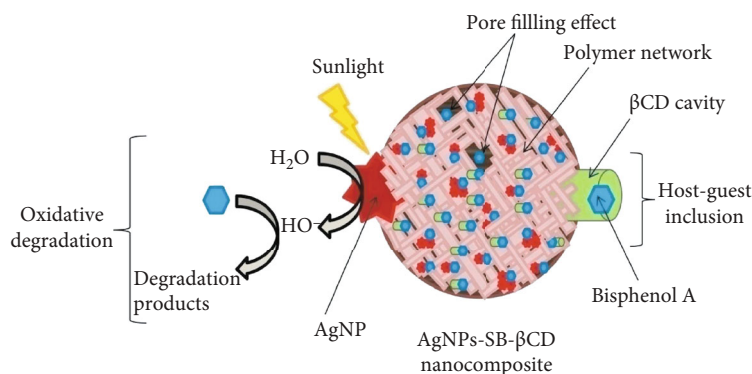


FIGURE 10: Illustration of the mechanisms for the BPA uptake onto AgNPs-SB- β CD.

3.3. Thermodynamic Study. Thermodynamic study stands as among the important analyses in adsorption process. This study can assist to know the adsorption behavior (nature) and temperature that suits adsorption interaction. As shown in Table 6, the negative Gibbs free change (ΔG^0) values imply the spontaneous compartment of adsorption phenomenon [26, 52]. Since all ΔG^0 values are less than -20 kJ mol^{-1} , the interaction of BPA and AgNPs-SB- β CD could be mostly controlled by physical adsorption [53] through host-guest inclusion (van der Waals bonding). Negative enthalpy change (ΔH^0) data suggests the exothermic character of the adsorption incident, while negative entropy change (ΔS^0) value indicates the lessening of degree of randomness at the interface of BPA and AgNPs-SB- β CD [44].

3.4. Regeneration Analysis. The tendency of an adsorbent to be reused for removing pollutant can promote its practical application and economical worth. This analysis can be used to confirm the stability and effectiveness of adsorbent on pollutant remediation [26, 54, 55]. According to the results, 75% ethanol had an uppermost desorption and regeneration ability of 72 and 95%, respectively, followed by 0.1 mol L^{-1} HCl solution. The slight lower desorption efficiency of AgNP-SB- β CD nanocomposites (72%) could be explained by the fact that not all BPA molecules presented in the aqueous solution were adsorbed via host-guest inclusion and pore filling mechanisms, but some were disintegrated (degraded) by the oxidative activity of AgNPs loaded onto bagasse-polymer. Therefore, this 72% could represent the BPA desorbed on AgNPs-SB- β CD from the total BPA concentration removed (adsorbed) by means of adsorption process. AgNP-SB- β CD nanocomposites have possessed a stable adsorption performance by not being affected greatly by desorption process and have demonstrated a great desorption and regeneration performances. Its regeneration capacity was lessened by 5% after five succeeding cycles. This confirms the market competition of AgNPs-SB- β CD towards remediation of wastewater tainted with BPA.

3.5. Adsorption and Oxidation Mechanisms. The surface features of AgNP-SB- β CD nanocomposites have played momentous roles in adsorption mechanisms. Figure 10 is a diagrammatic representation of the mechanism involved in the elimination of BPA from water matrix. The adsorbate-

adsorbent interaction mechanism was mainly operated by host-guest inclusion through involvement of van der Waals bonding. The 2' hydroxyl ($-\text{OH}$) groups on the beta-cyclodextrin (β -CD) cavities of AgNPs-SB- β CD were accountable for the uptake of bisphenol A through intermolecular hydrogen bonding and resulted the formation of inclusion complexes. These results are analogous to the findings reported by Ragavan et al. [56] and Mpatani et al. [26].

In addition to host-guest inclusion, pore diffusion effect has also participated in removing BPA from water matrix. The presence of mesopores (15.4 nm) on AgNP-SB- β CD surfaces had caused the diffusion of BPA into the interior part of polymeric nanocomposites; consequently, it brought adsorption process. On the other hand, oxidative dissolution of AgNPs embedded onto polymers has initiated the degradation of BPA. The dissolution incident of AgNPs assisted by poly(*N*-vinyl pyrrolidone) can trigger the generation of HO \cdot radicals in the sunlight's presence; as a result, it causes the decomposition of BPA through benzene ring cleavage [17, 57].

4. Conclusions

This research offers a comprehensive understanding on the greener synthesis of an innovative bagasse-polymer-silver nanocomposite adsorbent and its application in remediation of emerging micropollutant-bisphenol A (BPA) from water system. The process synthesis is reliable and sustainable and approaches on a cleaner and facile route. The impregnation of AgNPs onto bagasse-polymer material had increased the surface features (active sites/species, surface area, pore sizes, and cracks) and removal performance of polymeric nanocomposites towards BPA. The uptake of BPA onto AgNPs-SB- β CD is significantly dependent on the solution pH. In this present study, pH 7 had resulted the best removal performance due to the simultaneous occurrence of both adsorption and oxidative degradation processes. The kinetics and isotherms of adsorption followed pseudo-second-order and Langmuir models, respectively. The adsorption incident was governed mainly by physical adsorption via host-guest inclusion (van der Waals bonding) and pore filling effect. Besides, oxidative degradation had contributed marginally on the removal of BPA due to oxidative dissolution of AgNPs at pH 7. AgNP-SB- β CD had a maximum uptake capacity of 158.4 mg g^{-1} and was reused five times

without substantial loss on its efficiency. This novel AgNP-SB- β CD nanocomposite adsorbent had provided good removal capacity and higher steadiness on BPA compared to a number of adsorbents reported from the literature, consequently substantiates its practical application by offering a competition for BPA wastewater remediation.

Data Availability

All data generated and analyzed in this study are included within the article.

Additional Points

Highlights. (i) Novel AgNP-SB- β CD was fabricated to eliminate bisphenol A from aqueous matrix. (ii) AgNPs-SB- β CD had a highest uptake capacity of 158.4 mg g⁻¹ on bisphenol A. (iii) AgNP-SB- β CD possesses both adsorptive and oxidative properties on bisphenol A. (iv) AgNP-SB- β CD nanocomposites are stable and reusable; this promotes their market competition for remediation of BPA wastewater.

Conflicts of Interest

The authors declare that they have no competing interests.

Authors' Contributions

Farid Mzee Mpatani contributed to the supervision, conceptualization, methodology, formal analysis, investigation, writing—original draft, writing—review and editing, and visualization. Ussi Makame Kombo and Khamis Rashid Khair contributed to the methodology, formal analysis, investigation, and review and editing. Nahya Khamis Nassor, Daniel Joshua, Salma Saleh Mussa, Salama Abubakar Mohamed, Saide Abdulla Mbarak, Ali Shehe Hamad, and Salum Ali Ahmada contributed to the formal analysis and review and editing.

Acknowledgments

The authors acknowledge financial support by Tanzania Commission for Science and Technology (COSTECH) through MAKISATU (National Competition for Science, Technology and Innovation) program. Special thanks go to Nelson Mandela African Institution of Science and Technology (NM-AIST) and University of Dar es Salaam (UDSM), Tanzania, for characterization analysis. The authors also recognize Mr. Hassan Buda Juma (Data Manager) for his assistance on statistical analysis.

References

- [1] F. M. Mpatani, A. A. Aryee, A. N. Kani et al., "Removal of methylene blue from aqueous medium by citrate modified bagasse: kinetic, equilibrium and thermodynamic study," *Bioresource Technology Reports*, vol. 11, article 110463, p. 100463, 2020.
- [2] I. Ali, A. A. Basheer, X. Y. Mbianda et al., "Graphene based adsorbents for remediation of noxious pollutants from wastewater," *Environment International*, vol. 127, pp. 160–180, 2019.
- [3] C. A. Gasser, L. Yu, J. Svojitzka et al., "Advanced enzymatic elimination of phenolic contaminants in wastewater: a nano approach at field scale," *European journal of applied microbiology and biotechnology*, vol. 98, no. 7, pp. 3305–3316, 2014.
- [4] F. M. Mpatani, A. A. Aryee, A. N. Kani et al., "A review of treatment techniques applied for selective removal of emerging pollutant-trimethoprim from aqueous systems," *Journal of Cleaner Production*, vol. 308, article 127359, 2021.
- [5] M. Spadoto, A. P. E. Sueitt, C. A. Galinaro et al., "Ecotoxicological effects of bisphenol A and nonylphenol on the freshwater cladocerans *Ceriodaphnia silvestrii* and *Daphnia similis*," *Drug and Chemical Toxicology*, vol. 41, no. 4, pp. 449–458, 2018.
- [6] S. J. T. Gowder, "Nephrotoxicity of bisphenol A (BPA)—an updated review," *Current Molecular Pharmacology*, vol. 6, no. 3, pp. 163–172, 2013.
- [7] F. Maqbool, S. Mostafalou, H. Bahadar, and M. Abdollahi, "Review of endocrine disorders associated with environmental toxicants and possible involved mechanisms," *Life Sciences*, vol. 145, pp. 265–273, 2016.
- [8] A. Bhatnagar and I. Anastopoulos, "Adsorptive removal of bisphenol A (BPA) from aqueous solution: a review," *Chemosphere*, vol. 168, pp. 885–902, 2017.
- [9] I. Ali, "New generation adsorbents for water treatment," *Chemical Reviews*, vol. 112, pp. 5073–5091, 2012.
- [10] Q. Li, F. Pan, W. Li et al., "Enhanced adsorption of bisphenol A from aqueous solution with 2-vinylpyridine functionalized magnetic nanoparticles," *Polymers*, vol. 10, p. 1136, 2018.
- [11] J. Fan, W. Yang, and A. Li, "Adsorption of phenol, bisphenol A and nonylphenol ethoxylates onto hypercrosslinked and aminated adsorbents," *Reactive and Functional Polymers*, vol. 71, no. 10, pp. 994–1000, 2011.
- [12] J. Heo, Y. Yoon, G. Lee, Y. Kim, J. Han, and C. M. Park, "Enhanced adsorption of bisphenol A and sulfamethoxazole by a novel magnetic CuZnFe₂O₄-biochar composite," *Biore-source Technology*, vol. 281, pp. 179–187, 2019.
- [13] E. Dovi, A. N. Kani, A. A. Aryee et al., "Decontamination of bisphenol A and Congo red dye from solution by using CTAB functionalised walnut shell," *Environmental Science and Pollution Research*, vol. 28, no. 22, pp. 28732–28749, 2021.
- [14] S. Yüksel, N. Kabay, and M. Yüksel, "Removal of bisphenol A (BPA) from water by various nanofiltration (NF) and reverse osmosis (RO) membranes," *Journal of Hazardous Material*, vol. 263, pp. 307–310, 2013.
- [15] H. Zhang, Y. Wang, J. Wang, and Y. He, "Mechanism of bisphenol A removal by a submerged membrane bioreactor in the treatment of synthetic municipal sewage: staged analyses," *Desalination and Water Treatment*, vol. 57, no. 26, pp. 12364–12374, 2016.
- [16] M. Molkenhain, T. Olmez-Hanci, M. R. Jekel, and I. Arslan-Alaton, "Photo-Fenton-like treatment of BPA: effect of UV light source and water matrix on toxicity and transformation products," *Water Research*, vol. 47, no. 14, pp. 5052–5064, 2013.
- [17] C. M. Park, J. Heo, and Y. Yoon, "Oxidative degradation of bisphenol A and 17 α -ethinyl estradiol by Fenton-like activity of silver nanoparticles in aqueous solution," *Chemosphere*, vol. 168, pp. 617–622, 2017.

- [18] P. Guerra, M. Kim, S. Teslic, M. Alaei, and S. Smyth, "Bisphenol-A removal in various wastewater treatment processes: Operational conditions, mass balance, and optimization," *Journal of Environmental Management*, vol. 152, pp. 192–200, 2015.
- [19] R. Frankowski, A. Zgoła-Grześkowiak, W. Smulek, and T. Grześkowiak, "Removal of bisphenol A and its potential substitutes by biodegradation," *Applied Biochemistry and Biotechnology*, vol. 191, pp. 1100–1110, 2020.
- [20] F. M. Mpatani, R. P. Han, A. A. Aryee, A. N. Kani, Z. H. Li, and L. B. Qu, "Adsorption performance of modified agricultural waste materials for removal of emerging micro-contaminant bisphenol A: a comprehensive review," *Science of the Total Environment*, vol. 780, article 146629, 2021.
- [21] X. Xu, B. Y. Gao, B. Jin, and Q. Y. Yue, "Removal of anionic pollutants from liquids by biomass materials: a review," *Journal of Molecular Liquids*, vol. 215, pp. 565–595, 2016.
- [22] W. T. Tsai, C. W. Lai, and T. Y. Su, "Adsorption of bisphenol A from aqueous solution onto minerals and carbon adsorbents," *Journal of Hazardous Materials*, vol. 134, pp. 169–175, 2006.
- [23] Y. Wu, H. Qi, C. Shi, R. Ma, S. Liu, and Z. Huang, "Preparation and adsorption behaviors of sodium alginate-based adsorbent-immobilized β -cyclodextrin and graphene oxide," *RSC Advances*, vol. 7, no. 50, pp. 31549–31557, 2017.
- [24] S. Sonal and B. K. Mishra, "A comprehensive review on the synthesis and performance of different zirconium-based adsorbents for the removal of various water contaminants," *Chemical Engineering Journal*, vol. 424, article 130509, 2021.
- [25] M. R. Awual, T. Yaita, T. Kobayashi, H. Shiwaku, and S. Suzuki, "Improving cesium removal to clean-up the contaminated water using modified conjugate material," *Journal of Environmental Chemical Engineering*, vol. 8, no. 2, article 103684, 2020.
- [26] F. M. Mpatani, A. A. Aryee, A. N. Kani et al., "Uptake of micropollutant-bisphenol A, methylene blue and neutral red onto a novel bagasse- β -cyclodextrin polymer by adsorption process," *Chemosphere*, vol. 259, article 127439, 2020.
- [27] N. Pandey, S. K. Shukla, and N. B. Singh, "Water purification by polymer nanocomposites: an overview," *Nano*, vol. 3, pp. 47–66, 2017.
- [28] G. Lofrano, M. Carotenuto, G. Libralato et al., "Polymer functionalized nanocomposites for metals removal from water and wastewater: an overview," *Water Research*, vol. 92, pp. 22–37, 2016.
- [29] Y. Wu, H. Pang, Y. Liu et al., "Environmental remediation of heavy metal ions by novel-nanomaterials: A review," *Environmental Pollution*, vol. 246, pp. 608–620, 2019.
- [30] W. W. Tang, G. M. Zeng, and J. L. Gong, "Impact of humic/fulvic acid on the removal of heavy metals from aqueous solutions using nanomaterials: a review," *Science of the Total Environment*, vol. 468–469, pp. 1014–1027, 2014.
- [31] S. Daer, J. Kharraz, A. Giwa, and S. W. Hassan, "Recent applications of nanomaterials in water desalination: a critical review and future opportunities," *Desalination*, vol. 367, pp. 37–48, 2015.
- [32] N. A. Abdelwahab and N. Shukry, "Synthesis, characterization and antimicrobial properties of grafted sugarcane bagasse/silver nanocomposites," *Carbohydrate Polymers*, vol. 115, pp. 276–284, 2015.
- [33] M. L. F. A. De Castro, M. L. B. Abad, D. A. G. Sumalinog, R. R. M. Abarca, P. Paoprasert, and M. D. G. de Luna, "Adsorption of methylene blue dye and Cu (II) ions on EDTA-modified bentonite: isotherm, kinetic and thermodynamic studies," *Sustainable Environment Research*, vol. 28, pp. 197–205, 2018.
- [34] H. N. Tran, S.-J. You, A. Hosseini-Bandegharai, and H.-P. Chao, "Mistakes and inconsistencies regarding adsorption of contaminants from aqueous solutions: a critical review," *Water Research*, vol. 120, pp. 88–116, 2017.
- [35] M. A. Islam, M. R. Awual, and M. J. Angove, "A review on nickel(II) adsorption in single and binary component systems and future path," *Journal of Environmental Chemical Engineering*, vol. 7, no. 5, article 103305, 2019.
- [36] B. Doczekalska, K. Kusmierk, A. Swiatkowski, and M. Bartkowiak, "Adsorption of 2,4-dichlorophenoxyacetic acid and 4-chloro-2-methylphenoxyacetic acid onto activated carbons derived from various lignocellulosic materials," *Journal of Environmental Science and Health, Part B*, vol. 53, pp. 290–297, 2018.
- [37] D. Paramelle, A. Sadovoy, S. Gorelik, P. Free, J. Hobley, and D. G. Fernig, "A rapid method to estimate the concentration of citrate capped silver nanoparticles from UV-visible light spectra," *Analyst*, vol. 139, pp. 4855–4861, 2014.
- [38] I. Fernando and Y. Zhou, "Impact of pH on the stability, dissolution and aggregation kinetics of silver nanoparticles," *Chemosphere*, vol. 216, pp. 297–305, 2019.
- [39] K. Jyoti, M. Baunthiyal, and A. Singh, "Characterization of silver nanoparticles synthesized using *Urtica dioica* Linn. leaves and their synergistic effects with antibiotics," *Journal of Radiation Research and Applied Sciences*, vol. 9, no. 3, pp. 217–227, 2016.
- [40] V. T. Trinh, T. M. P. Nguyen, H. T. Van et al., "Phosphate adsorption by silver nanoparticles-loaded activated carbon derived from tea residue," *Scientific Reports*, vol. 10, p. 3634, 2020.
- [41] P. Prakash, P. Gnanaprakasam, R. Emmanuel, S. Arokiyaraj, and M. Saravanan, "Green synthesis of silver nanoparticles from leaf extract of *Mimusops elengi*, Linn. for enhanced antibacterial activity against multi drug resistant clinical isolates," *Colloids and Surfaces B: Biointerfaces*, vol. 108, pp. 255–259, 2013.
- [42] R. P. Han, Y. Wang, Q. Sun et al., "Malachite green adsorption onto natural zeolite and reuse by microwave irradiation," *Journal of Hazardous Materials*, vol. 175, no. 1–3, pp. 1056–1061, 2010.
- [43] A. A. Aryee, F. M. Mpatani, Y. Y. Du et al., "Fe₃O₄ and iminodiacetic acid modified peanut husk as a novel adsorbent for the uptake of Cu (II) and Pb (II) in aqueous solution: characterization, equilibrium and kinetic study," *Environmental Pollution*, vol. 268, no. Part A, article 115729, 2021.
- [44] C. Y. Kuo, "Comparison with as-grown and microwave modified carbon nanotubes to removal aqueous bisphenol A," *Desalination*, vol. 249, pp. 976–982, 2009.
- [45] B. O. Orimolade, F. A. Adekola, and G. B. Adebayo, "Adsorptive removal of bisphenol A using synthesized magnetite nanoparticles," *Applied Water Science*, vol. 8, no. 1, p. 46, 2018.
- [46] Z. Zhao, D. Fu, and B. Zhang, "Novel molecularly imprinted polymer prepared by palygorskite as support for selective adsorption of bisphenol A in aqueous solution," *Desalination and Water Treatment*, vol. 57, pp. 12433–12442, 2016.
- [47] Y.-K. Choi and E. S. Kan, "Effects of pyrolysis temperature on the physicochemical properties of alfalfa-derived biochar for

- the adsorption of bisphenol A and sulfamethoxazole in water,” *Chemosphere*, vol. 218, pp. 741–748, 2019.
- [48] V. Ponnusami, V. Gunasekar, and S. N. Srivastava, “Kinetics of methylene blue removal from aqueous solution using gulmohar (*Delonix regia*) plant leaf powder: Multivariate regression analysis,” *Journal of Hazardous Materials*, vol. 169, no. 1-3, pp. 119–127, 2009.
- [49] A. N. Kani, E. Dovi, A. A. Aryee et al., “Polyethyleneimine modified tiger nut residue for removal of Congo red from solution,” *Desalination and Water Treatment*, vol. 215, pp. 209–221, 2021.
- [50] C. Levard, S. Mitra, T. Yang et al., “Effect of chloride on the dissolution rate of silver nanoparticles and toxicity to *E. coli*,” *Environmental Science & Technology*, vol. 47, no. 11, pp. 5738–5745, 2013.
- [51] S. Garg, H. Y. Rong, C. J. Miller, and T. D. Waite, “Oxidative dissolution of silver nanoparticles by chlorine: implications to silver nanoparticle fate and toxicity,” *Environmental Science & Technology*, vol. 50, no. 7, pp. 3890–3896, 2016.
- [52] L. Ai, C. Zhang, and Z. Chen, “Removal of methylene blue from aqueous solution by a solvothermal-synthesized graphene/magnetite composite,” *Journal of Hazardous Materials*, vol. 192, pp. 1515–1524, 2011.
- [53] R. Kumar, J. Rashid, and M. A. Barakat, “Synthesis and characterization of a starch–AlOOH–FeS₂nanocomposite for the adsorption of Congo red dye from aqueous solution,” *RSC Advances*, vol. 4, no. 72, pp. 38334–38340, 2014.
- [54] A. A. Aryee, E. Dovi, R. P. Han, Z. H. Li, and L. B. Qu, “One novel composite based on functionalized magnetic peanut husk as adsorbent for efficient sequestration of phosphate and Congo red from solution: characterization, equilibrium, kinetic and mechanism studies,” *Journal of Colloid and Interface Science*, vol. 598, pp. 69–82, 2021.
- [55] J. L. Wang, X. Liu, M. M. Yang et al., “Removal of tetracycline using modified wheat straw from solution in batch and column modes,” *Journal of Molecular Liquids*, vol. 338, article 116698, 2021.
- [56] K. V. Ragavan and N. K. Rastogi, “ β -Cyclodextrin capped graphene-magnetite nanocomposite for selective adsorption of Bisphenol-A,” *Carbohydrate Polymers*, vol. 168, pp. 129–137, 2017.
- [57] R. Broséus, S. Vincent, K. Aboufadel et al., “Ozone oxidation of pharmaceuticals, endocrine disruptors and pesticides during drinking water treatment,” *Water Research*, vol. 43, pp. 4707–4717, 2009.